The 8/5 resonance between TRAPPIST-1 innermost planets

C. Charalambous[1,2] & C. Beaugé[1,2]

[1] *Instituto de Astronomía Teórica y Experimental, CONICET–UNC, Argentina*
[2] *Observatorio Astronómico de Córdoba, UNC, Argentina*

Contact / ccharalambous@unc.edu.ar

Resumen / La interacción entre los planetas y el disco protoplanetario produce que éstos migren a una tasa que depende de las características del disco de gas y la masa de los planetas migrantes. Debido a la incerteza en la determinación de las masas de los planetas del sistema TRAPPIST-1, sus tasas de migración no están bien determinadas. En este trabajo presentamos el resultado de simulaciones de N-cuerpos con migración de tipo I para reproducir la configuración general de TRAPPIST-1 y estudiar su estado multiresonante. Encontramos que la escala de tiempo de circularización orbital, caracterizada mediante el factor de decaimiento de la excentricidad Q_e, es un parámetro crítico para reproducir su arquitectura. Si $Q_e < 0.1$ la órbita se circulariza más rápidamente y es posible encontrar una captura en la resonancia de movimientos medios 8/5 entre los dos planetas más internos.

Abstract / Interactions between the planets with the protoplanetary gas disk produce migration, whose rates depend on the features of the gas-disk and the mass of the migrating planets. Due to the uncertainties in the estimations of masses of the TRAPPIST-1 planets, their migration rates are not well determined. In this work, we present N-body simulations including type-I migration, to reproduce the general configuration of the TRAPPIST-1 system and analyze its multi-resonant state. We found that the circularization timescale, characterized by the Q_e eccentricity damping factor, is a critical parameter in reproducing its architecture. When $Q_e < 0.1$ the orbit circularizes faster and we are able to find resonance trapping in the 8/5 mean motion resonance between the two innermost planets.

Keywords / planet–disk interactions — protoplanetary disks — celestial mechanics

1. Introduction

TRAPPIST-1 (Gillon et al., 2016, 2017) is a transiting planetary system orbiting an ultra-cool dwarf star. The star (with an age of 7.6 ± 2.2 Gyrs, Burgasser & Mamajek, 2017) hosts a compact system of seven planets on the super-Earth regime in a complex resonant chain comprised of five interlocked zero-order 3-body mean-motion resonances (MMRs), Luger et al. (2017).

It is currently accepted that during the first stages of planetary formation a gaseous disk existed, and protoplanets were embeded in it. Interactions between the gas disk and the embryos produce a loss of angular momentum in the planet that makes it migrate inwards (Ward, 1997). The torque that the planet is immersed to depends on the features of the disk, and is inversely proportional to its mass. Throughout this process, planets are expected to get trapped in 2-planet (2P-) MMRs. A resonant relation is satisfied by the mean motions n_i of the planets when $pn_1 - (p+q)n_2 \sim 0$ with $p, q \in \mathbb{Z}$, and the associated resonant angle $\phi_{1,2} \sim p\lambda_1 - (p+q)\lambda_2 + q\varpi_{1,2}$ will librate around a fixed value, with λ_i the mean longitudes and ϖ_i the longitudes of perihelion. The main problem for understanding the dynamical evolution of TRAPPIST-1 is that the masses of the planets are estimated with great uncertainties (see Table 1) implying that we can not delimit the migration rates. This is important because depending on the speed with which the planet overpasses the resonance, it might get captured or continue its orbital decay towards the central star.

Table 1: Relative mass, $\mu_i \equiv m_i/m_\oplus$, of each planet i of the TRAPPIST-1 system, estimated by Gillon et al. (2017) assuming the central star mass is $m_\star = m_\odot$.

μ_b	μ_c	μ_d	μ_e	μ_f	μ_g
10.62 $\pm$ 9	17.25 $\pm$ 7.62	5.12 $\pm$ 3.37	7.75 $\pm$ 7.25	8.5 $\pm$ 2.25	16.75 $\pm$ 11

In Charalambous et al. (2018) we presented dynamical maps in the $(n_1/n_2, n_2/n_3)$ representative plane and used them to understand the TRAPPIST-1 architecture. By N-body simulations including type-I migration, we managed to reproduce most 3-planet subsystems in their observed double resonances, except for one. We could never recover the b-c-d location because the b-c pair never achieved the 8/5 MMR. In this work, we focus on reproducing the b-c resonant configuration.

2. Migration prescriptions

Tanaka et al. (2002) developed a linear theory considering the gravitational interaction between a small planet and a 3D isothermal gaseous disk, described by a power-law surface density $\Sigma(r)$ and disk aspect ratio $h(r)$:

$$\Sigma(r) = \Sigma_0 (r/r_0)^{-\alpha} \quad , \quad h(r) = h_0 (r/r_0)^f, \qquad (1)$$

where Σ_0 and h_0 are the values at $r_0 = 1\,au$, and α is the slope of the surface density profile. The disk is char-

acterized by different values for f, a parameter known as flare index. If $f = 0$ the disk is flat while for $f > 0$, it is flared (Bitsch et al., 2013).

Assuming that there was a single planet in the system in a non eccentric orbit and with no inclination with respect to the disk mid plane, Tanaka et al. (2002) proposed an analytical formula for the orbital decay timescale τ_a. The expression for the i-th planet with mass m_i orbiting around a star of mass $m_\star$ is given by

$$\tau_{a_i} = \frac{Q_a t_{\mathrm{w}_i}}{h(r_i)^2}, \qquad t_{\mathrm{w}_i} = \frac{m_\star}{m_i}\frac{m_\star}{\Sigma(r_i) r_i^2}\frac{h(r_i)^4}{\Omega(r_i)}, \tag{2}$$

with $\Sigma(r_i)$ given in Equation (1), $\Omega(r_i)$ the Keplerian angular velocity, and $Q_a^{-1} \simeq 2.7 + 1.1\alpha$. Equation (2) show that the migration timescale is proportional to the planet-to-star mass-ratio, the position of the migrating planet, and the disk local features.

Tanaka & Ward (2004) considered the low eccentricity case and propose a circularization timescale, then modified by Cresswell & Nelson (2006) to fit hydrodynamic multiplanet simulations using an eccentricity damping factor Q_e. Thus, the time τ_e needed for a planet in an isothermal disk to damp its eccentricity is

$$\tau_{e_i} = Q_e \frac{t_{\mathrm{w}_i}}{0.78}\left[1 + \frac{1}{4}\left(\frac{e_i}{h(r_i)}\right)^3\right], \tag{3}$$

with the ad-hoc fixed parameter $Q_e = 0.1$, and being e_i the eccentricity of planet i.

3. The 8/5 mean-motion resonance

Planets b and c of TRAPPIST-1 are supposed to reside in an 8/5 commensurability. For resonance trapping to be possible in a 2-planet system, it is necessary that their relative migration is convergent. This means that the outer planet has to migrate faster than the inner one ($\tau_{a_i} > \tau_{a_{i+1}}$). There are different combinations for the TRAPPIST-1 system that allow $\tau_{a_b} > \tau_{a_c}$. We maintain fixed the mass of planet c and all disk parameters, except for α and f. Results are shown in Figure 1, the dashed line indicates where migration goes from convergent (above) to divergent (beneath).

We varied μ_b between the lower possible estimated value 1.62 (see Table 1) up to the mean value for $\mu_c = 17$. Default values for disk parameters were $f = 0$, and $\alpha = 0.5$ (see Charalambous et al. (2017) for details in the election of this values). It follows from Equations (2) and (3) that migration timescales will be modified.

In the top panel of Figure 1 we varied the disk flare index $f \in [0, 1]$, and in the lower panel the exponent of the power-law surface density α between $[0.5, 1.5]$. Results suggest that given a value for μ_b, different f and α can generate conditions for convergent or divergent migration scenarios. If TRAPPIST-1 had been born in a flat laminar disk, the range of values $\mu_b = [1.62, 17]$ is possible. However, if the nascent disk had a more flared shape, say $f = 1$, we should never get any resonant trapping for $\mu_b \gtrsim 6$ because migration gets divergent. Limit masses for convergent migration of the intermediate disks lay between this values. The α parameter shows a similar situation, although divergence appears for larger mass-ratios ($\mu_b \gtrsim 12$).

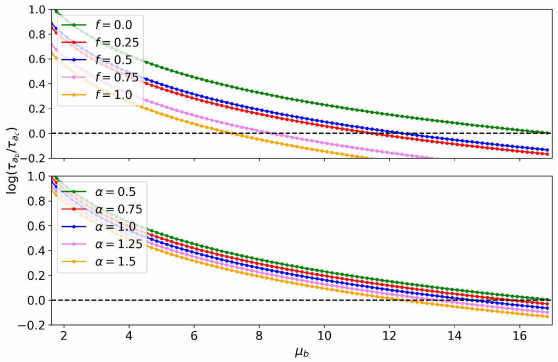

Figure 1: Migration timescales ratio as a function of the mass of the inner planet, calculated with Equation (2). Default values were chosen as $f = 0$ and $\alpha = 0.5$. For the mass of planet b we explored the range of values provided in Table 1 $\mu_b = [1.62, 17]$, and for the mass of planet c we set $\mu_c = 17$. The dashed line indicates where migration goes from convergent (above) to divergent (beneath). *Top panel:* variation of the disk flare index $f \in [0, 1]$. *Bottom panel:* exponent of the surface density $\alpha \in [0.5, 1.5]$.

However, as explained in Ramos et al. (2017), relative differential migration rates should be slow enough to increase the probability of capture, which is only possible if the mass-ratio is close to unity. If the disk-driven planetary migration is sufficiently slow and smooth, the orbits remain almost circular and it is expected that the system gets captured in resonance. This implies that the mass of planet b should be close to the mass of planet c. Convergent migration for $\mu_b/\mu_c \approx 1$ is seen in Figure 1 for flat disks and with low α.

4. Reproduction of the complete architecture

In order to reproduce the 8/5 MMR between planets b and c, we made N-body simulations with the migration prescriptions presented in Equations (2) and (3), and integrated for $5{\times}10^5$ years. We varied the mass of planet b and the masses of planets c to h were fixed in the values with which resonant capture was attained in Charalambous et al. (2018): $\mu_c = 17$, $\mu_d = 17.6$, $\mu_e = 18.4$, $\mu_f = 19.5$, $\mu_g = 21$ and $\mu_h = 24$.

We used for the inner planet $\mu_b \in [16, 17]$, and the parameters for the disk were $f = 0$, $\alpha = 0.5$, $h_0 = 0.03$, and $\Sigma_0 = 50\,\mathrm{gr\,cm^{-2}}$. Results were interpreted using the $\max(\Delta a) = \max(\Delta a_i)$ dynamical maps presented in Charalambous et al. (2018), where $\Delta a_i = (a_{i_{\max}} - a_{i_{\min}})$ represent the variation in the semimajor-axis, a_i. However, none of this parameters generated a successful capture for inner triplet in the representative plane. The double resonance $(3/2, 5/3)$ was always achieved.

A different way of analyzing the resonant captures is by modifying the circularization timescale, which depends on all the disk parameters and the mass of the migrating planet: $\tau_{e_i} \propto Q_e/m_i$. In Charalambous (2020) we changed τ_e through the artificial Q_e damping factor. We investigated a set of 10 different values for $Q_e \in [0.05, 0.15]$, centered in the number proposed by Cresswell & Nelson (2006).

Typical outcomes for values of $Q_e \geqslant 0.1$ are sim-

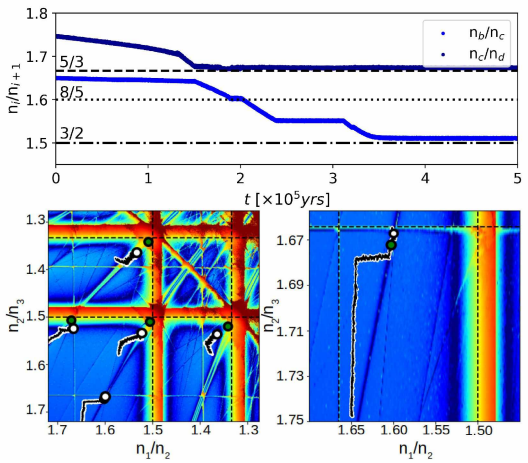

Figure 2: *Top panel:* Example of a migration simulation with $\mu_b = 16.8$ and $Q_e = 0.12$. *Bottom panels:* Background: max(Δa) dynamical map. Superimposed: N-body simulation including type-I planetary migration of a TRAPPIST-1-like system with the same μ_b but $Q_e = 0.07$. The *bottom-left* panel shows the general trend of the system while the *bottom-right panel* shows a zoom of the *b*-*c*-*d* sub-system. Green dots represent the observed position of each triplet while the white circles depict the final state of the simulation, see chapter 6 of Charalambous (2020) for further details.

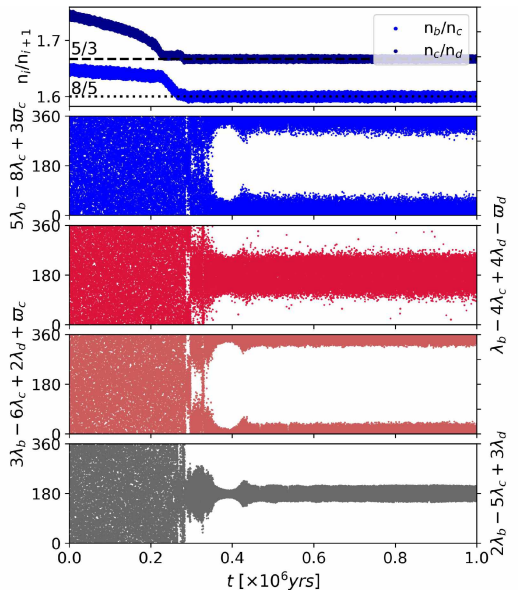

Figure 3: From top to bottom: n_i/n_{i+1} as a function of time, and 2 and 3-planet resonant angles for a system with $\mu_b = 16.7$ and $Q_{e_b} = 0.09$, $Q_{e_c} = 0.063$, $Q_{e_d} = 0.098$.

ilar to that represented in the top panel of Figure 2, a temporal brief capture and escape of the 8/5 MMR. However, an example of a simulation with $Q_e = 0.07$ is shown in the lower frames of Figure 2, were we obtained a permanent capture in the 8/5 MMR. Nevertheless, the outer triplets display higher offsets than the observed ones, and those obtained in Charalambous et al. (2018) and Charalambous (2020). In the simulations, initial semimajor axis for each planet was set to a value larger than currently observed, specifically: $a_b = 0.18$ au, $a_c = 0.25$ au, $a_d = 0.36$ au, $a_e = 0.49$ au, $a_f = 0.66$ au, $a_g = 0.8$ au and $a_h = 1.11$ au, and all initial eccentricities were fixed in $e_i = 0.01$.

To address this issue, here we refined the Q_e space to understand the 2P-MMRs deeply for fixed values of μ_b. We performed new sets of 200 simulations, with slightly different initial conditions for Q_{e_i} chosen randomly for each of the three inner planets, allowing different circularization timescales for each body. Integrations with lower Q_{e_i} need less time to circularize the orbit. Thus, the planets spend more time in near circular orbits and captures get favored. In all cases, the outer pair reached the 5/3 resonance regardless of whether the innermost was captured, either temporarily or permanently, in the 8/5 MMR. Figure 3 shows the 8/5 MMR between planets b and c ($\phi_{b,c}$ is shown in blue librating around $5\lambda_b - 8\lambda_c + 3\varpi_c$) and the 3-planet MMR angles librating, both for zeroth and first order, for a simulation with $\mu_b = 16.7$ and $Q_{e_b} = 0.09$, $Q_{e_c} = 0.063$, $Q_{e_d} = 0.098$, extended for 10^6 years.

5. Conclusions

Although the approach chosen for this study is not the conventional one to investigate the planet disk interactions problem, the circularization timescale τ_e depends on the Q_e factor. When we maintain fixed all features of the disk and vary Q_e, the time it takes for a planet to circularize its orbit changes. Moreover, this timescale is different for different planets. We understand this as a variation on the physical properties of the disk because all other free parameters are fixed. For the TRAPPIST-1 particular problem, we found that for $Q_e \geqslant 0.1$ it takes more time to dampen eccentricities and resonant captures never occurred, but they do for $Q_e < 0.1$.

The amount of temporal and permanent captures for $Q_e \simeq 0.05$ is around 40%, and diminishes to less than 15% while Q_e grows for all the masses studied. Our study of the TRAPPIST-1 system shows that its nascent disk may have been more complex than previously thought. The efficiency of permanent trapping is not clear though, and requires further analysis.

Acknowledgements: This work has been supported by research grants from CONICET and Secyt-UNC, and used computational resources from CCAD (https://ccad.unc.edu.ar/).

References

Bitsch B., et al., 2013, A&A, 549, A124
Burgasser A.J., Mamajek E.E., 2017, ApJ, 845, 110
Charalambous C., 2020, , Ph.D. thesis, UNC
Charalambous C., et al., 2017, *JPCS*, vol. 911, 012027
Charalambous C., et al., 2018, MNRAS, 477, 1414
Cresswell P., Nelson R.P., 2006, A&A, 450, 833
Gillon M., et al., 2016, Nature, 533, 221
Gillon M., et al., 2017, Nature, 542, 456
Luger R., et al., 2017, Nat. Astron., 1, 0129
Ramos X.S., et al., 2017, A&A, 602, A101
Tanaka H., Takeuchi T., Ward W.R., 2002, ApJ, 565, 1257
Tanaka H., Ward W.R., 2004, ApJ, 602, 388
Ward W.R., 1997, Icarus, 126, 261